X International Conference on Computational Methods in Marine Engineering
MARINE 2023
J. Garcia-Espinosa, L. González, J.E. Gutiérrez & B. Serván-Camas (Editors)

Scale effect in the self-propulsion prediction for Ultra Large Container Ship with contra-rotating propellers

MARINE 2023

Hanna Pruszko[1*], Maciej Reichel [2] , Krzysztof Czerski[3] , Marek Necel[3], Julia Schmale[4] and Sören Brüns[4]

[1] Gdańsk University of Technology, Faculty of Mechanical Engineering and Ship Technology, ul. Gabriela Narutowiczan11/12, 80-233 Gdańsk, Poland, web: https://wimio.pg.edu.pl/en/homepage

[2] Prof. Lech Kobyliński Foundation for Safety of Navigation, Ship Handling and Training Research Center 14-200 Iława - Kamionka, Poland, web: https://www.ilawashiphandling.com.pl

[3] Seatech Engineering sp z o.o. ul. Plac Porozumienia Gdańskiego 1, 80-864 Gdańsk, Poland, web: https://www.seatech.com.pl

[4]Hamburgische Schiffbau-Versuchsanstalt GmbH, Bramfelder Str. 164, 22305 Hamburg, Germany, web: https://www.hsva.de/

[*] Corresponding author: Hanna Pruszko, hanna.pruszko1@pg.edu.pl

ABSTRACT

This article addresses the problem of the scale effect for an Ultra Large Container Ship (ULCS) with a novel twin-crp-pod propulsion system. Twin-crp-pod steering-propulsion arrangement is an innovative solution that gains from three well-known systems: twin-propeller, contra-rotating propellers and pod propulsors. It is expected that applying the twin-crp-pod system to the analysed Ultra Large Container Ship will increase propulsion efficiency and manoeuvring safety. To prove that, a series of model tests have been carried out, including towing tank tests and free-sailing manoeuvring tests.

The scope of the presented simulations included calm water resistance simulations and self-propulsion tests for the full-scale and model-scale vessels. The model-scale calculations have been performed at a scale of 1:37.416. During self-propulsion simulations, the required front and aft propeller revolutions were searched to find the optimum power balance. Calculations were performed for the ship design speed and constant front-to-aft propeller revolutions ratio. The case study vessel was a 400m Ultra Large Container Ship. CFD Simulations were performed using the unsteady RANS approach. The sliding mesh approach with a rotating region around the local coordinate system was used to model the propeller directly. The flow was turbulent with the k-ω SST turbulence model applied. The second-order implicit temporal discretisation scheme was applied.

Parallel, due to the early stage of research, an extrapolation method including the wake scaling, propellers interactions and pod housing resistance is being elaborated. Later on, the model-scale CFD results will be extrapolated and compared to the results of the full-scale simulations. As for now, the comparison included the total resistance of the bare hull, wake fraction, relative rotational efficiency, thrust deduction and propeller revolution required to achieve the self-propulsion point.

Keywords: extrapolation method; CFD computations; hybrid crp-pod.

NOMENCLATURE

J	Advance coefficient[-]
K_T	Thrust coefficient [-]
K_Q	Torque coefficient [-]
P_D	Total delivered power [W]
R_T	Total resistance [N]
Q	Propeller Torque [Nm]
T	Propeller Thrust [N]
t	Thrust deduction [-]
w	Wake fraction [-]
η_0	Propeller efficiency [-]
η_R	Rotational efficiency [-]
CFD	Computational Fluid Dynamics

1. INTRODUCTION

Reduction of fuel consumption and minimisation of greenhouse gas emissions are vital now for the shipping industry. All possible ways to achieve environmental targets should be taken into consideration. Conventional propellers are known to have low efficiency. Most ship propellers on cargo vessels waste about 40 per cent of the energy in the form of rotational losses in the wake, vortex generation, noise production, cavitation, etc. The recovery of such losses is one of the major ways to contribute to a more rational, environmentally friendly use of energy.

Ultra-large container ships are those that, on the one hand, have individually the highest carbon footprint. On the other hand, take advantage of economy of scale and transport vast amounts of goods worldwide. Therefore, this type of ship is a perfect target for taking action to investigate energy-efficient solutions. Twin-crp-pod propulsion arrangement is an innovative solution that gains from three well-known systems: twin-propeller, contra-rotating propellers and pod propulsors. Such a combination should guarantee an increase in efficiency, loss of GHG emissions and improvement of manoeuvrability and ship handling abilities.

All three ideas that will be developed and combined in the project are well known. Twin propeller configuration has been utilised for years for ships with draft restrictions, where the required power is too large to be consumed by one propeller with limited diameter. Podded propulsors are used especially on ships with high manoeuvrability requirements, like cruise ships, icebreakers or offshore vessels. Contra rotating propellers concept in classic form, i.e. two propellers on a shaft, is also a known solution for reducing fuel consumption for containerships, bulk carriers or crude carriers.

There are designs that combine two of mentioned solutions, e.g. hybrid crp-pod, where a single pod propulsor is placed behind a conventional propeller and works on the contra rotation principle (Sánchez-Caja et al. 2013; Quereda et al. 2017; Petteri 2004; Sasaki et al. 2009). Such a configuration has been introduced to high-speed vessels, like ro-pax (Ueda et al. 2004). The studies of the CRP-POD propulsion efficiency were carried out by (Chang and Go 2011; Ying et al. 2016). Z. Wang et al. (2021) compared the self-propulsion performance of the CRP-POD vessel and single screw ship. Moreover, the design optimisation, such as the propeller design parameters and clearance between the propellers, were investigated (Zhanzhi Wang, Xiong, and Wang 2016; Zhang et al. 2019).

These investigations have been carried out, whether employing model tests or CFD computations. Model tests from their nature and CFD computations in most cases from the reason of time and cost efficiency are carried out in model scale. Thus, the propulsion prediction for the actual ship requires a reliable method for full-scale extrapolation. The common knowledge is that the aft propeller has little influence on the front propeller. This

has been reported, e.g. by (Sasaki et al. 2009; Go, Seo, and Chang 2005; Quereda et al. 2017). Wang et al. (2016), while studying the scale effect in the prediction of the hydrodynamic performance of crp-pod vessels, presented, however, some new insights. The authors noticed that not only does the pod resistance change along with the Reynolds number and forward/aft propellers revolution ratio, but also the thrust and torque coefficients change nearly linearly with this ratio.

An essential contribution to the crp-pod propulsion prediction in terms of a proposal for an extrapolation method has been made by (Quereda et al. 2017) and (Chang and Go 2011). Both methods are based on the ITTC-78 method, but the latter takes the axial suction effect due to the aft propeller for scaling of wake fraction into account. However, there are still some issues that have to be investigated deeper. Some of these are the scaling of the aft propeller's wake, the pod housing's frictional resistance, the scaling of open water characteristics of the aft propeller, and the optimum power balance between the aft/fore propeller for the model and full scale.

Therefore, the presented investigation has aimed to find out how the scale influences the before-mentioned issues and to elaborate, based on CFD computations, a comprehensive and reliable extrapolation method for propulsion prediction. Various scales have been considered, and one of them, together with full-scale computations, is presented (Reichel et al., 2022).

2. METHODS

2.1 Case Study Vessel

The case study vessel was an Ultra Large Container Ship. The hull was redesigned, starting from the single screw ship. The decision process and redesigning objectives to obtain the twin screw model of the single screw hull were described in detail by (Reichel et al. 2022).

The pod housing was designed based on the analysis of the currently available market solutions. The choice of the propeller geometry parameters was based on the literature review and case study propellers were chosen from the stock propellers database of Prof. Lech Kobyliński Foundation for Safety of Navigation and Gdańsk University of Technology. Table 1 presents the main particulars of the case study vessel. The scale of 1:37.416 was chosen for the purpose of future validation against the towing tank tests.

Table 1. Main particulars of the case study vessel.

Name	Symbol	Value – Full Scale	Value – Model Scale
Length overall	LOA	399.90 m	10.11 m
Length between perpendiculars	LPP	378.4 m	10.69 m
Breadth moulded	B	53.60 m	1.433 m
Draught (scant.)	T_S	16.00 m	0.428 m
Drought (design)	T_D	14.00 m	0.374 m
Displacement	∇_D	199068 m^3	3.80 m^3
Service speed	V_S	21 kn (10.8 m/s)	1.766 m/s

Figure 1 presents the 3D model of the twin-screw bare hull and aft part of the ship equipped with the pods and propellers.

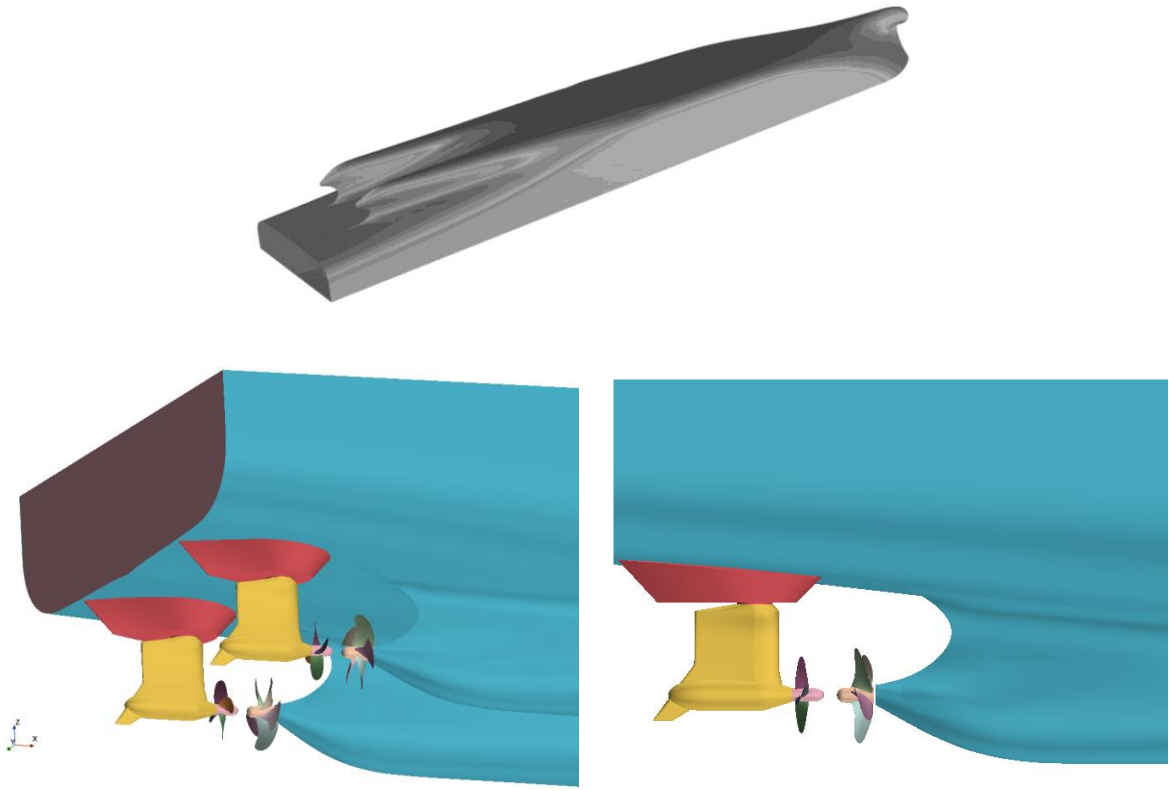

Figure 1. The hull shape, pod and propellers of ULCS with twin-crp-pod propulsion

Table 2 presents the geometry parameters of the front and aft propellers.

Table 2. Propeller geometry parameters full scale/model scale

Name	Symbol	Front propeller	Aft propeller
Diameter	D	7.68 m /0.205 m	6.00 m /0.16 m
Number of blades	Z	5	4
Pitch Ratio	P/D	1.0221	1.016
Expanded area ratio	A_E/A_0	0.8014	0.5184

2.2 Numerical Simulations

Numerical methods allow us to solve discretised governing equations of mass, momentum and energy conservation, commonly known as Navier-Stokes equations. Depending on the problem, different simplifications might be applied. For naval applications, where fluid is assumed to be incompressible, only mass and momentum continuity is considered. However, the significant complexity of flow around a ship hull does not allow for solving equations analytically and numerical methods need to be applied.

The calculations were done by means of URANS simulations. The finite volume method was applied to solve the governing equations of mass and momentum conservation, and Star CCM+ software was used. The flow was solved as three-dimensional, turbulent, viscous, incompressible and multiphase. The RANS approach is based on the assumption that instantaneous velocity might be represented by the sum of mean and fluctuating components. Those values are then averaged and inserted into N-S equations. Averaging process involves introducing additional terms that increase the number of unknown values in RANS equations. In this study, different turbulence models were applied depending on the simulation type.

The scope of numerical simulation included:

- Open water propeller simulations – evaluation of K_T, K_Q, η *vs* J plot –**model** scale and **full** scale
- Calm water resistance simulations – for a design speed of 21 knots (corresponding to 1.766 m/s in model scale) – **model** scale and **full** scale
- Self-propulsion simulations – for a design speed of 21 knots (corresponding to 1.766 m/s in model scale), a constant ratio of revolution between front and aft propellers and two different sets of propellers RPM – **model** scale and **full** scale

Therefore, three different set-ups of numerical simulations were applied: to evaluate open-water propeller characteristics, calm water simulations, and assess the self-propulsion point. The differences included mesh, temporal discretisation, and computational domain size. Following subsections aim to describe in detail the set-up of each simulation type.

2.2.1 Open-water propeller simulations

The open water propeller characteristics assessment followed standard procedure and guidelines (ITTC, 2011, 2014) (Siemens PLM Software, 2017). The calculations were performed for the range of advance ratio J between 0.3 and 1.0 with 0.1 increments, constant propeller revolution and varying values of water inflow velocity. The steady solver was used, and 1000 iterations were performed for each value of J was required to obtain convergence of thrust and torque. The rotating reference frame was applied.

The size of the computational domain was equal to 10D × 5D × 5D, where D is the diameter of the propeller. The propeller was placed 4D behind the upstream boundary plane and 6D in front of the downstream boundary. The velocity inlet and pressure outlet boundary conditions were prescribed for upstream and downstream boundaries, respectively. The remaining boundaries had symmetry plane conditions.

The size of the mesh was 4.72 M cells; 4.3 M cells were in the rotating region around the propeller, whereas the rest were in the background far-field region. The rotating region around the propeller had a size of 1.3D. Special attention was put to meshing the tips of the propeller resulting in the minimum size of the element being equal to 0.02% D. In the area of the boundary layer region, the prism cells were applied, and the total thickness of the prism layer was 5e-5 m for the model scale, and 0.001 m for full scale. With 5 layers and a stretch factor equal to 1.5, the resulting y+ was kept below 3 for model scale simulation and above 30 in full-scale simulation. The final result of the simulation was open-water propeller characteristics.

2.2.2 Calm water simulations

The size of the domain and ship position was specified to capture the Kelvin wave pattern and avoid reflection from the side and downstream boundary. For the same reason, numerical wave damping was applied to these boundaries. For the full-scale simulations, the length of the computation domain was 4 L_{OA} m, the breadth was 1.5 L_{OA} m, and it was 1.7 L_{OA} high. The upstream boundary was located 1 L_{OA} from the ship's bow, and the

downstream boundary was 2 L_{OA} behind the ship. The top and bottom boundary was located 0,7 L_{OA} and 1 L_{OA} from the ship, respectively. The side boundary was located 1.5 L_{OA} from the ship.

The velocity inlet condition was applied to the upstream, top, and bottom boundaries. The symmetry condition was applied to side boundaries, and the pressure outlet condition was assigned to the downstream boundary. It was decided that only half of the model would be taken for the computations (symmetry plane condition). For model scale simulations, the entire domain was scaled by 1:37.416 to obtain the model scale corresponding to towing tank experiments.

The time step of numerical simulations varied accordingly to vessel speed to satisfy the Courant-Friedrich's-Lewy condition, defined by Equation 1. In the formula, Δt stands for a time step, Δx is a grid size in the direction of a flow velocity vector, u is velocity, and C is constant. For naval applications, it is recommended that C is equal to 0.5 – 0.7 for free surface and 5-10 for hull surface (Siemens PLM Software 2017).

$$\frac{u \cdot \Delta t}{\Delta x} \leq C \tag{1}$$

In order to capture the interface between phases, a surface-capturing VOF (Volume of Fluid) model was applied. The k–ε model with all y+ treatments was applied for simulations. This model offers a good compromise between robustness and accuracy. The model is also a frequent choice when using STAR CCM+ software (Kim et al. 2017; Tezdogan et al. 2015). Four degrees of freedom were restrained, and the model was allowed to sink and trim. To compute the motions of a ship as a response to fluid forces, the DFBI model (Dynamic Fluid Body Interaction) was applied. This module allows to integrate pressure and shear forces over the surface of a body. Acting forces and moments are used to find the new position of an object iteratively after translational motion and angular rotation of the body centre of mass (Siemens PLM Software 2017).

The discretisation of the volume was performed according to a recent state-of-the-art. Grid refinements were applied to make it possible to capture essential features of the flow. It included increasing mesh resolution in the free surface, wake and the closest proximity to the hull surface where prism layers were used in the region of the boundary layer. For the model scale, the y+ below 2 was obtained for most of the cells, whereas for full-scale computation, the mesh resolution in the region of the ship boundary layer resulted in a value of y+ within a range of 100-150. The approach with the symmetry plane of a ship was used, and the total number of volumetric cells was equal to 5.6 M cells.

2.2.3 Self-propulsion simulations

The size of the numerical domain and boundary conditions were the same as for the calm water simulations. The mesh resolution for self-propulsion simulations was very similar to calm water simulations. However, the differences obviously included the volume around the propellers. Two separate rotating regions were generated around each propeller, and a sliding mesh approach was used. There was an interface boundary condition between the static region containing the hull, pod housing, and far-field area and regions around the propellers. The propeller mesh resolution was similar to the one described in Section 2.2.1. Due to additional refinement in the static region around the volume containing rotating regions and the presence of pod housing, the final mesh count was equal to 5.6 M cells in the static region, 5.4 M cells in the rotating region of the front propeller and 2.7 M cells in the second rotating region containing the aft propeller. The final mesh resolution is presented in Figure 2.

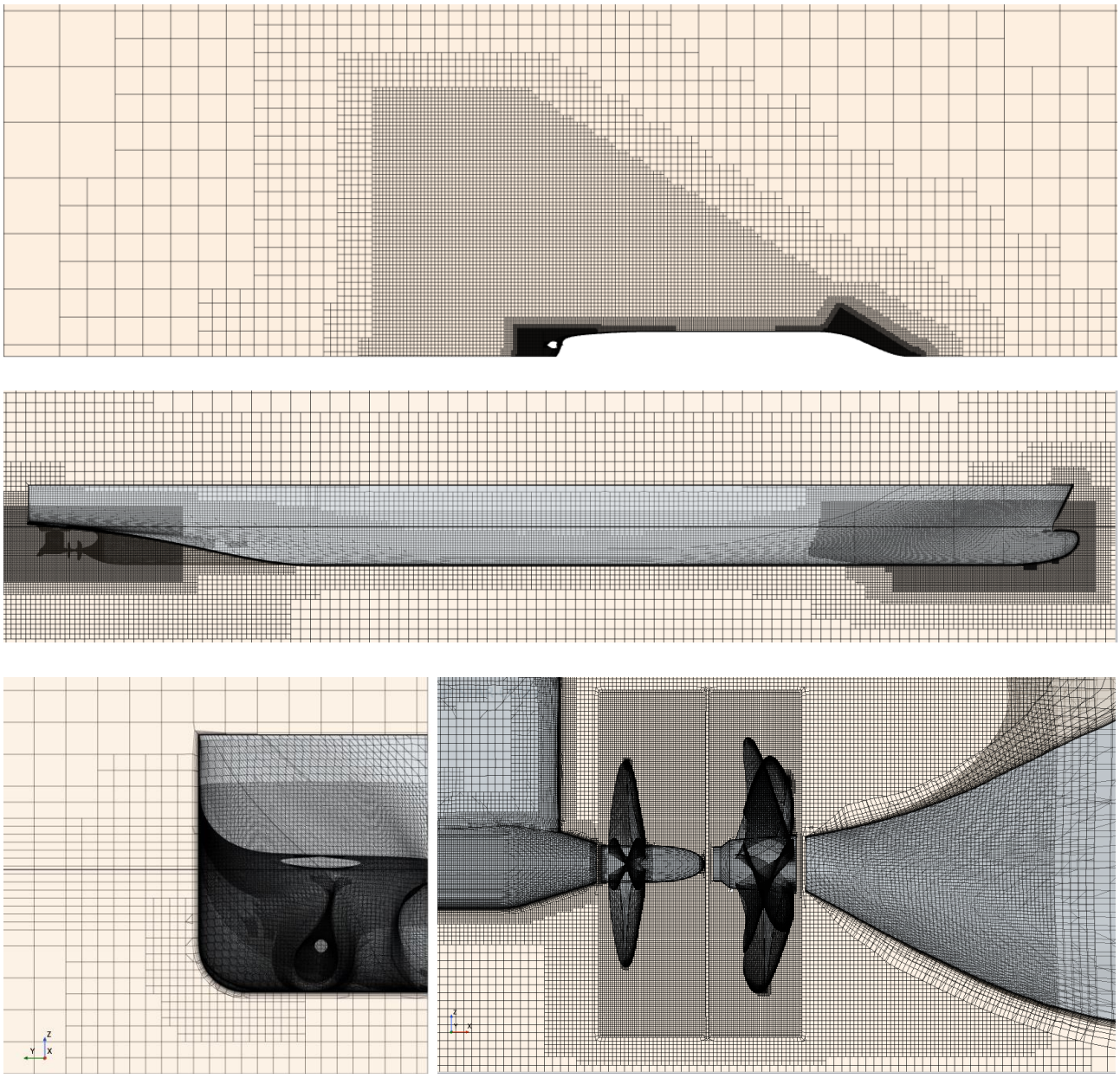

Figure 2. The numerical mesh

Since it is quite a common choice for propeller simulations, the k-ω SST turbulence model was chosen (Ponkratov and Zegos 2015). The second-order implicit temporal discretisation scheme was applied. The time step was equal to 0.005 s for full-scale simulations and $9 \cdot 10^{-4}$ s for model-scale simulations. For both scales, it corresponds to more than 100 time steps per propeller rotation for the highest value of analysed pod propeller RPM. The front and aft propeller revolution ratio was kept constant, and it was equal to 1.26. The revolution of propellers was changed to obtain the required thrust and, therefore, to find the self-propulsion point. Table 3 presents the summary of the self-propulsion computation cases.

Table 3. Propeller revolution parameters full scale/model scale

	Point 1	Point 2
Front propeller RPS (model scale)	8.0	8.5
Aft propeller RPS (model scale)	10.08	10.71
Front propeller RPM (full scale)	78.5	85.8
Aft propeller RMM (model scale)	98.9	108.1

The values that were evaluated from the numerical simulations were the total resistance of the hull, pod housing, propellers thrust and torque, and net force (calculated as the difference between total resistance and combined thrust of propellers). For the model scale simulation, the friction deduction force was equal to 44.5 N and included in the calculations.

2.3 Scale effect assessment

The aim of the article is to compare the different aspects of hull propeller interaction, which are defined in this section. The result of the calm water simulation is the total resistance of the ship, together with the thrust of the propeller. It allows us to calculate the thrust deduction defined in Eq. 2 as:

$$t = \frac{T - R_T}{T} \tag{2}$$

Directly from the self-propulsion trials, one can obtain the thrust and torque of the propellers at some particular revolution rate n that corresponds to the self-propulsion point. Based on that, it is possible to obtain thrust and torque coefficients according to Eq. 3:

$$K_T = \frac{T}{\rho n^2 D^4};\ K_Q = \frac{Q}{\rho n^2 D^5} \tag{3}$$

Once the values of the thrust and torque coefficients from self-propulsion trials are known from the open water propeller characteristics, it is possible to read the propeller advance coefficient during the trials and assume the thrust identity, also the rotational efficiency defined in Eq. 4 as:

$$\eta_R = \frac{K_{Q0}}{K_{QB}} \tag{4}$$

Where K_{QB} is the torque coefficient from the self-propulsion trials, and K_{Q0} is the value of the torque coefficient in the open water condition. Based on advance ratio J, the inflow velocity to the propeller is calculated as presented in Eq. 5:

$$V_A = JnD \tag{5}$$

Then, the wake fraction is calculated according to Eq. 6:

$$w = \frac{V_S - V_A}{V_S} \tag{6}$$

Those formulae were used to determine the influence of the hull on the propellers and *vice versa*, and using them, the interaction of hull and propeller in model and full scale were compared.

3. Results

3.1 Open water propeller characteristics

The open-water propeller characteristics were evaluated in both scales for the front and aft propellers. The results for the front propeller are presented in Figure 3. The full scale is presented on the left plot model scale and the right hand.

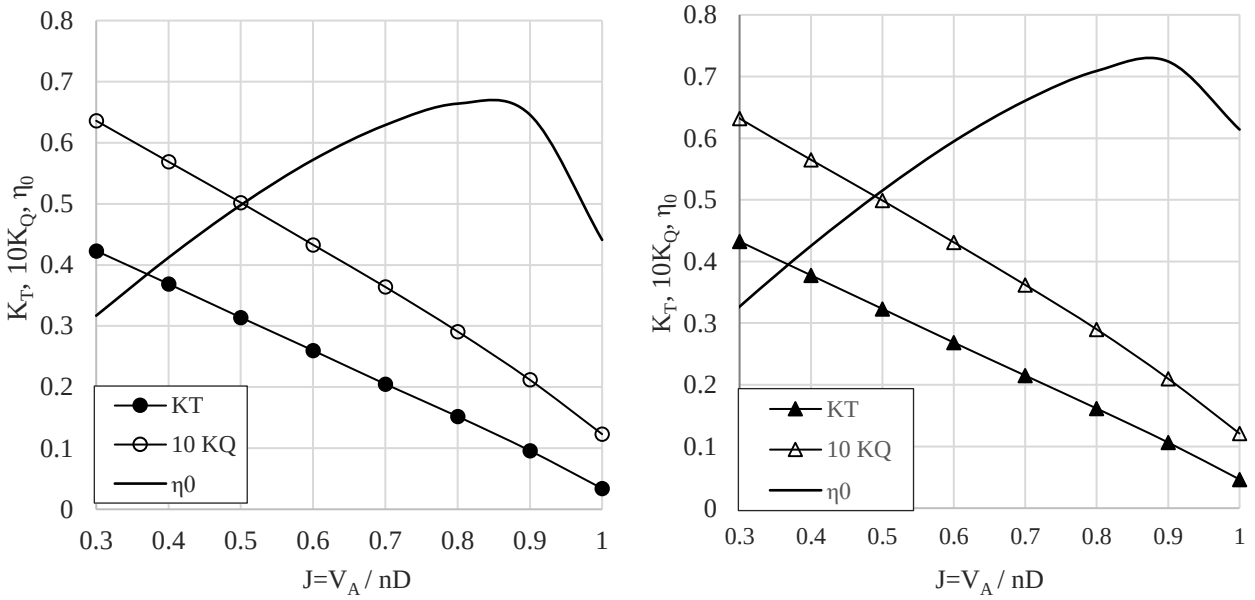

Figure 3. Front propeller open water characteristics in model scale (left) and full scale (right)

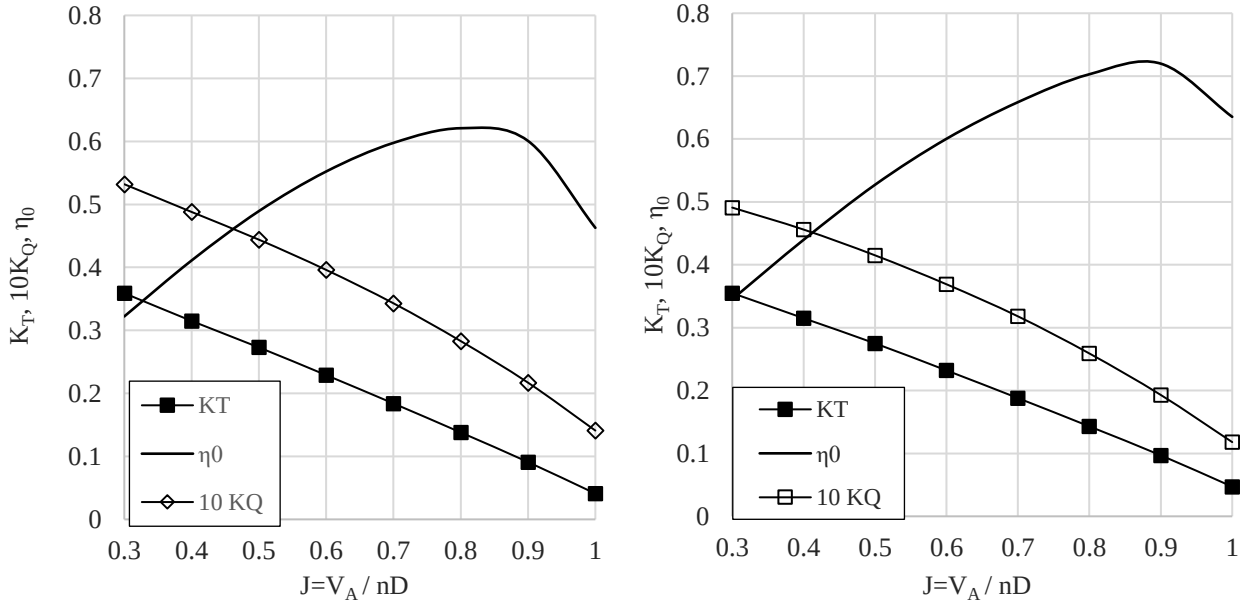

Figure 4. Front propeller open water characteristics in model scale (left) and full scale (right)

The results for the aft propeller are presented in Figure 4. Similarly, the results for the model scale are presented on the left and the right for the full scale. The open-water propeller characteristics were used to evaluate the wake fractions of propellers and relative rotational efficiency according to formulae presented in Section 2.3

3.2 Calm water resistance

The calculation of the total resistance in the model and full scale were performed with the rudders. The numerical uncertainty was estimated to be equal to 0.9%. In Table 4, the results of both scale numerical simulations are presented.

Table 4. Results of the calculations – calm water resistance

Name	CFD – model scale	CFD – full
C_T	$3.13 \cdot 10^{-3}$	$1.70 \cdot 10^{-3}$
C_P	$6.10 \cdot 10^{-4}$	$3.03 \cdot 10^{-4}$
C_F	$2.52 \cdot 10^{-3}$	$1.40 \cdot 10^{-3}$
Trim	0.05 deg	0.04 deg
Sinkage/L	$7.02 \cdot 10^{-4}$	$7.11 \cdot 10^{-4}$

It can be noticed that the results for trim and sinkage agree well with each other. Therefore, there is no significant scale effect. It is evident for friction forces. However, it is surprising to find high differences in the pressure resistance coefficient. Nevertheless, since the calculations were performed for the Froude number $F_N = 0.176$, the influence on total resistance is relatively small.

3.3 Self-propulsion calculations

For the self-propulsion calculations, first, from the linear interpolation, the self-propulsion point needs to be estimated. To do that, the relation between the front propeller revolution and the net force was plotted. The point where it intersects the X-axis is the self-propulsion point. The remaining quantities: thrust and torques of the propellers are calculated based on that. For the model scale simulations, the values of the net force, aft propeller revolution, thrusts and torques of both propellers vs the revolution of the front propeller are presented in Figure 5 on the left side. The analogous plot for the full-scale simulations is presented on the right side of Figure 5. The black arrows indicate the self-propulsion point. Based on the obtained values of thrust and torque of both propellers, the coefficients describing propeller-hull interaction were evaluated. Those values are summarised in Table 5.

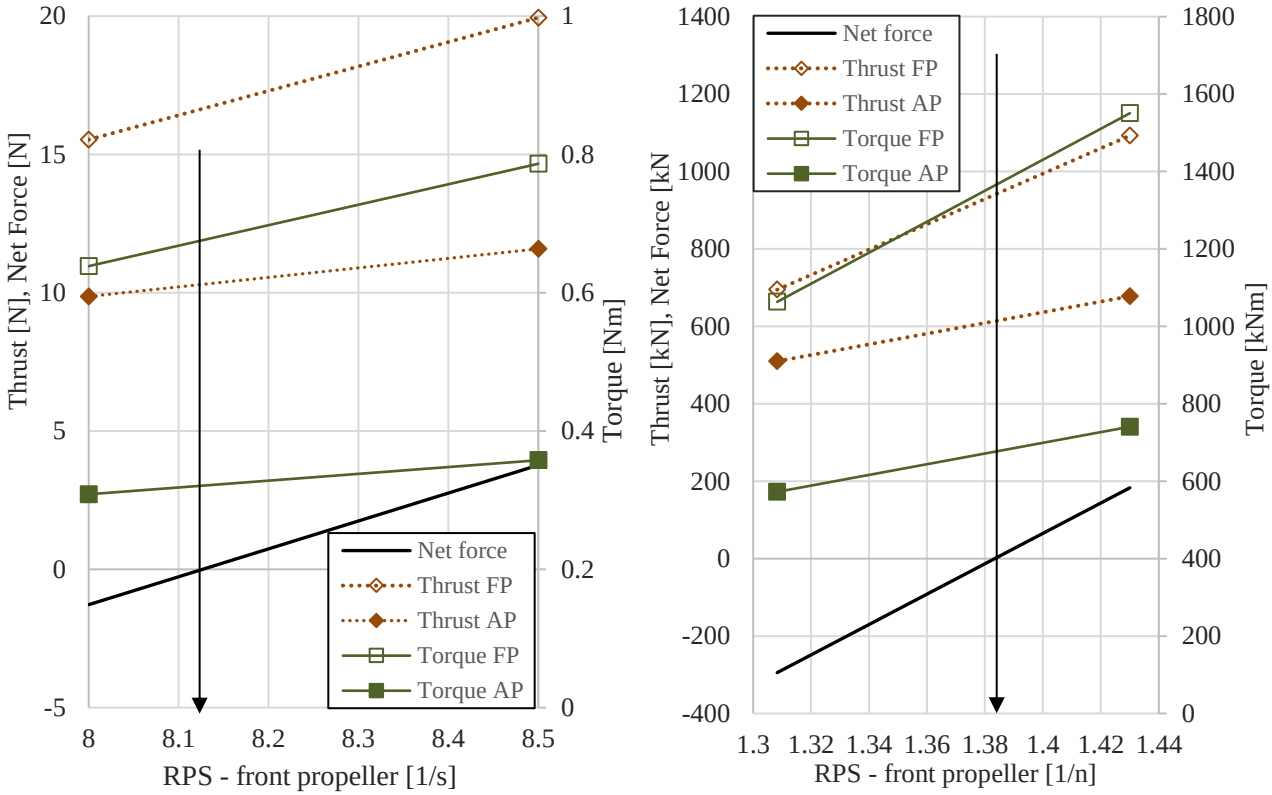

Figure 5. Self-propulsion point evaluation

Table 5. Results of the calculations – model scale and full scale

	CFD Model Scale		CFD Full Scale	
	Front propeller	Aft propeller	Front propeller	Aft propeller
RPS/RPM	8.13	10.24	83.8	105.6
K_T	0.143	0.151	0.142	0.156
J	0.811	0.768	0.833	0.765
K_{QB}	0.0283	0.0293	0.0267	0.0289
K_{Q0}	0.0275	0.0307	0.0259	0.280
η_0	0.65	0.62	0.71	0.69
η_R	0.97	1.03	0.97	0.97
w	0.235	0.278	0.181	0.260
t	0.107		0.215	

4. DISCUSSION

In this section, some considerations about the obtained results are included. According to Figure 3 and Figure 4, the full-scale propellers are characterised by higher efficiency than the model-scale propellers. This is in line with the ITTC correction that are modifying mainly the torque coefficient for full-scale extrapolation. The increase in torque values in the model scale is especially pronounced for the aft propeller.

According to Figure 5, the self-propulsion point is obtained for revolutions of the front propeller equal to

8.13 RPS and the corresponding revolution of the aft propeller is equal to 10.24 RPS. For the model scale, the self-propulsion point is obtained for the front propeller revolution equal to 1.397 PRS, and the aft propeller revolution equal to

1.76 RPS. From the plot, the thrust and torque of the propellers can also be read.

According to Table 5, the values of K_T are very similar for both scales, with less than a one per cent difference between each other. From the open water propeller curve based on the calculated values of K_T, the advance coefficients were calculated. Values of front propeller advance coefficients are slightly different, whereas, for aft propellers, they are very close to each other in both scales. According to expectations, the values of torque coefficient K_{QB} for model scale propellers are greater. Also, the values of propeller torque coefficients K_{Q0} are greater in the model scale.

The aspects that require a bit more attention are values of relative rotational efficiency, thrust deduction and wake fraction. It is not clear why the relative rotational efficiency for pod propeller changed to unfavourable for full-scale cases, and it would require deeper investigation. For the front propeller, the wake fraction in the model scale is significantly more significant than in the full scale, and it could be easily explained by the different thicknesses of the boundary layer in the model and full scale. What is more interesting is that for the aft propeller, the wake fractions differ very slightly from each other. It seems that the presence of the rotating propeller upstream from the other one mitigates the problem of different thickness boundary layers, as it is no longer crucial for the inflow velocity profile to the aft propeller. Therefore, it seems that the wake correction for the aft propeller in extrapolation calculations seems redundant. Lastly, the most surprising is the thrust deduction which is much greater for a full scale, although it is typically considered to be the same in model and full scale. This aspect will be more closely investigated, possibly for other scales, and a more systematic numerical study will be conducted to assess the uncertainty of this estimation. It will include a time step, mesh and turbulence model sensitivity study. Obtained results will also be compared with model test results.

5. CONCLUSIONS

This article addressed the problem of scale effect for self-propulsion calculations of the vessel with the hybrid twin contra-rotating pod propulsion system. The study aimed to quantify and compare the coefficients describing the hull–propeller interaction in two scales: the model scale of 1:37.416 and the full scale. The case study vessel was a 400 m long Ultra Large Container Ship. The goal of the study was achieved, and performed calculations allowed us to draw several important conclusions.

The most important findings apply to wake fraction and thrust deduction. For the aft propeller, the wake fractions were found to be almost the same. Therefore, the wake correction for the aft propeller seems to be unnecessary. Second, significant differences between the thrust deduction factors in both scales occurred. This is very different from the general assumption of equal thrust deduction in the model and full scale. Therefore, it will be investigated in detail in the future. This study is a novelty considering that such a propulsion system has not been widely investigated before, and systematic studies on the scale effect for contra-rotating propellers are limited.

The future works will focus on validating the results and detailed numerical verification study to confirm presented very interesting findings.

ACKNOWLEDGEMENTS

This work was supported by MarTERA and co-financed by Polish National Centre for Research and Development (NCBR) and Development (NCBR) under the grant agreement MARTERA-2/twin-crp-pod ULCS/1/2020 and the German Federal Ministry of Economic Affairs and Energy (BMWi).

Calculations were carried out at the Centre of Informatics Tricity Academic Supercomputer & Network.

REFERENCES

Chang, Bong Jun, and Seokcheon Go. 2011. "Study on a Procedure for Propulsive Performance Prediction for CRP-POD Systems." *Journal of Marine Science and Technology* 16 (1). https://doi.org/10.1007/s00773-010-0108-8.

Go, Seokcheon, Heungwon Seo, and Bong Jun Chang. 2005. "On the Model Tests for POD Propulsion Ships." *Journal of Ship and Ocean Technology* 9 (1).

Kim, Yoo Chul, Kwang Soo Kim, Jin Kim, Yoonsik Kim, Il Ryong Park, and Young Hun Jang. 2017. "Analysis of Added Resistance and Seakeeping Responses in Head Sea Conditions for Low-Speed Full Ships Using URANS Approach." *International Journal of Naval Architecture and Ocean Engineering* 9 (6): 641–54. https://doi.org/10.1016/j.ijnaoe.2017.03.001.

Petteri, Ämmälä. 2004. "CRP Azipod Propulsion Concept-Advanced Cost-Effective Solution." *Journal of The Japan Institute of Marine Engineering* 39 (9). https://doi.org/10.5988/jime.39.544.

Ponkratov, Dmitriy, and Constantinos Zegos. 2015. "Validation of Ship Scale CFD Self-Propulsion Simulation by the Direct Comparison with Sea Trials Results." In *Fourth International Symposium on Marine Propulsors*. Texas.

Quereda, Ramón, Mariano Pérez-sobrino, Juan González-adalid, and Cristina Soriano. 2017. "Conventional Propellers in CRP-POD Configuration . Tests and Extrapolation ." *Proceedings of the Fifth International Symposium on Marine Propulsors*, no. June.

Reichel, Maciej, Hanna Pruszko, Krzysztof Czerski, and Marek Necel. 2022. "Innovative Twin-Crp-Pod Propulsion System for Ultra Large Container Ships - Challenges and Opportunities." In *15th International Symposium on Practical Design of Ships and Other Floating Structures PRADS 2022*.

Sánchez-Caja, Antonio, M Pérez-Sobrino, R Quereda, M Nijland, T Veikonheimo, J González-Adalid, Ilkka Saisto, and A Auriarte. 2013. "Combination of Pod, CLT and CRP Propulsion for Improving Ship Efficiency: The TRIPOD Project." In *Proceedings of the Third International Symposium on Marine Propulsors SMP '13*.

Sasaki, Noriyuki, Mariko Kuroda, Junichi Fujisawa, Takanori Imoto, and Masaharu Sato. 2009. "On the Model Tests and Design Method of Hybrid CRP Podded Propulsion System of a Feeder Container Ship." In *First International Symposium on Marine Propulsors*.

Siemens PLM Software. 2017. "User Guide Star CCM+ V12.04."

Tezdogan, Tahsin, Yigit Kemal Demirel, Paula Kellett, Mahdi Khorasanchi, Atilla Incecik, and Osman Turan.

2015. “Full-Scale Unsteady RANS CFD Simulations of Ship Behaviour and Performance in Head Seas Due to Slow Steaming.” *Ocean Engineering* 97: 186–206. https://doi.org/10.1016/j.oceaneng.2015.01.011.

Ueda, Naoki, Akira Oshima, Takashi Unseki, Shigetomo Fujita, Shingen Takeda, and Tohru Kitamura. 2004. “The First Hybrid CRP-POD Driven Fast ROPAX Ferry in the World.” *Technical Review* 41 (6).

Wang, Zhan-zhi, Min Shao-song, Peng Fei, and Shen Xing-rong. 2021. “Comparison of Self-Propulsion Performance between Vessels with Single-Screw Propulsion and Hybrid Contra-Rotating Podded Propulsion.” *Ocean Engineering* 232. https://doi.org/https://doi.org/10.1016/j.oceaneng.2021.109095.

Wang, Zhan Zhi, Ying Xiong, Rui Wang, and Chen Hua Zhong. 2016. “Numerical Investigation of the Scale Effect of Hydrodynamic Performance of the Hybrid CRP Pod Propulsion System.” *Applied Ocean Research* 54. https://doi.org/10.1016/j.apor.2015.10.006.

Wang, Zhanzhi, Ying Xiong, and Rui Wang. 2016. “Effect of the Main Design Parameters on the Open-Water Performance of a Hybrid CRP Podded Propulsion System.” *Harbin Gongcheng Daxue Xuebao/Journal of Harbin Engineering University* 37 (1). https://doi.org/10.11990/jheu.201410034.

Ying, Xiong, Zhang Ke, Wang Zhan-zhi, and Qi Wan-jiang. 2016. “Numerical and Experimental Studies on the Effect of Axial Spacing on Hydrodynamic Performance of the Hybrid CRP Pod Propulsion System *.” *China Ocean Eng* 30 (4): 627–36. https://doi.org/10.1007/s13344-016-0040-8.

Zhang, Yu Xin, Xiao Ping Wu, Zhi Yong Zhou, Xuan Kai Cheng, and Yu Long Li. 2019. "A Numerical Study on the Interaction between Forward and Aft Propellers of Hybrid CRP Pod Propulsion Systems." *Ocean Engineering* 186. https://doi.org/10.1016/j.oceaneng.2019.05.066.